

Effect of neutron irradiation on the density of low-energy excitations in vitreous silica

T. L. Smith, P. J. Anthony, and A. C. Anderson

Department of Physics and Materials Research Laboratory, University of Illinois at Urbana-Champaign, Urbana, Illinois 61801

(Received 23 December 1977)

Neutron irradiation of vitreous silica produces changes of the same relative magnitude in the low-temperature excess specific heat C_{ex} , the anomalous thermal conductivity κ , and the anomalous temperature dependence of ultrasonic velocity, $\Delta v/v$. It is therefore likely that κ and $\Delta v/v$ are dominated by the localized excitations responsible for the excess specific heat of vitreous silica. The tunneling-states model with a single energy-dependent density of states adequately accounts for the measured C_{ex} , κ , and $\Delta v/v$ of unirradiated vitreous silica. Changes in these properties with neutron irradiation can be explained using this model by altering only the density of tunneling states.

I. INTRODUCTION

The low-temperature properties of amorphous materials are distinct from those of crystalline dielectrics and are remarkably independent of the detailed atomic composition of the materials. For temperatures $T \lesssim 1$ K, the specific heat is much larger than the T^3 Debye term contributed by phonons.¹ This excess specific heat, which varies roughly as T , arises from a broad spectrum of localized low-energy excitations.² Presumably these excitations are intrinsic to the amorphous structure.

The theoretical problem is to provide a description of the localized excitations. Several models have been suggested to explain the excess specific heat.³⁻⁹ The difficulty lies in explaining how a localized vibration can have an extremely broad range of resonant frequencies, $\approx 10^6$ – 10^{12} Hz, with the motion localized¹⁰ to a region of diameter $\lesssim 20$ Å. The model that is most successful envisions the localized excitations to be associated with the quantum-mechanical tunneling of some entity between two configurations of nearly equal potential energy.^{11,12} This model will be discussed in greater detail in Sec. II.

The thermal conductivities of glassy materials vary roughly as T^2 below ≈ 1 K and have a region of weaker temperature dependence (a "plateau") near 10 K. Heat is transported by acoustical thermal phonons² which are scattered strongly by some mechanism characteristic of all amorphous systems. The tunneling-states model can account for the observed T^2 temperature dependence, although it has been argued that scattering mechanisms other than localized excitations should be present in a noncrystalline dielectric.^{3,8,13-20} Phonon scattering has also been studied using ultrasonic measurements. Only the tunneling-states theory has, thus far, been applied to the saturation (reduction) in attenuation with increased

acoustical intensity²¹ and the occurrence of phase coherence as observed in phonon echoes.²²

Thus, the tunneling-states model for the localized excitations can explain qualitatively the variety of unusual low-temperature properties found in amorphous materials, even though a physical description of the tunneling entity is not available for any material. A quantitative comparison between this theory and experiment is hampered by a lack of empirical information. For example, it is not known what fraction of phonon scattering in thermal transport is caused by localized excitations and what fraction by other mechanisms. Further, for that scattering caused by localized excitations, there is some question as to what fraction of the total spectrum of excitations is involved, since only those having a relatively short relaxation time should contribute strongly to phonon scattering. Hence, various subsets of localized excitations may be involved in different physical properties. The purpose of the work reported here is to provide some of this information.

It was expected from earlier work that neutron irradiation of vitreous silica would reduce the number of localized excitations in such a manner that the amorphous nature of the silica would not be lost.²³⁻²⁵ The earlier work showed that irradiation increased the thermal conductivity²⁶ and decreased the specific heat²⁷ at low temperatures. We have therefore made systematic measurements of specific heat, thermal conductivity, and ultrasonic velocity on both neutron-irradiated and unirradiated samples cut from a single piece of vitreous silica. The experimental techniques used are described in Sec. III.

The results, discussed in detail in Sec. IV, suggest that the low-temperature properties of unirradiated vitreous silica can be explained adequately by localized excitations alone. Moreover, the changes due to neutron irradiation in specific

heat, thermal conductivity, and ultrasonic velocity appear to have a common origin, namely, a change in the density of localized excitations. In comparing our results with the tunneling-states model, we find good agreement using a single energy-dependent density of states to explain all properties. This is true not only in the range $T \lesssim 1$ K, for which the model was developed, but also at higher temperatures. However, we do not intend to imply that the tunneling-states model provides a unique explanation for the localized excitations.

II. TUNNELING-STATES MODEL

The tunneling-states model is discussed extensively in the existing literature.^{11, 12, 21, 28, 29} We therefore present here only a general outline of the theory plus those details and extensions pertinent to the ensuing discussion.

The tunneling-states model envisions that some units of the glass reside in double-well potentials as shown schematically by the inset in Fig. 1. The weak overlap of the ground-state wave functions in the two individual minima, plus the asymmetry ϵ between these minima, give rise to a small energy splitting E between the ground state and the first excited state of the combined system. The splitting is given by $E = (\Delta^2 + \epsilon^2)^{1/2}$, where the overlap energy Δ varies with the well separation $2d$, the height V of the potential energy barrier, and the mass m of the tunneling unit.

In principle, one could obtain a density of tunneling states²⁸ $P(\epsilon, \lambda)$ in terms of the double-well parameters ϵ and λ . [The parameter $\lambda = (2mV)^{1/2}$

d/\hbar is proportional to $\ln \Delta$.] Experimentally, however, the density $P(E, \tau)$ is more accessible, where τ is the relaxation time of a tunneling state of energy E . It has been suggested²¹ that τ arises primarily through a modulation $\delta\epsilon$ in the asymmetry ϵ by the strain e of a passing acoustical phonon. Assuming the coupling parameter $\gamma = \delta\epsilon/2e$ is essentially independent²¹ of E , then²⁸

$$\tau^{-1} = \sum_i \left(\frac{2\gamma^2}{\rho v^2} \right)_i (4\pi\hbar^4 v_i^3)^{-1} \Delta^2 E \coth(E/2kT), \quad (1)$$

where ρ is the mass density, v is the acoustical-phonon velocity, and the summation is over the three acoustical-phonon modes. In the past, it has generally been assumed for convenience that $P(\epsilon, \lambda)$ is a constant independent of ϵ and λ . In the present paper, however, we shall allow $P(\epsilon, \lambda) = P(E)$, which has at most only a weak dependence on τ . Then,²⁸

$$P(E, \tau) = (2\tau)^{-1} (1 - \tau_{\min}/\tau)^{-1/2} P(E), \quad (2)$$

where $\tau_{\min} = (\Delta/E)^2 \tau$ is the shortest relaxation time that occurs in the sample for states of energy E .

Several physical properties are now calculated. The specific heat is given by

$$C_{\text{ex}} = \int_0^{E_{\max}} dE E^2 [4kT^2 \cosh^2(E/2kT)]^{-1} \times \int_{\tau_{\min}}^{\tau_{\max}} d\tau P(E, \tau) \quad (3)$$

$$= \int_0^{E_{\max}} dE E^2 [4kT^2 \cosh^2(E/2kT)]^{-1} P(E) \eta(E), \quad (4)$$

where $\eta(E)$ represents²⁹ the quantity $\frac{1}{2} \ln(4\tau_{\max}/\tau_{\min})$. Note that the time scale t of the experiment determines τ_{\max} if the distribution over τ extends to that time scale. If $P(E)$ is a constant P_0 ,

$$C_{\text{ex}} = \left(\frac{1}{6} \pi^2 k^2 \right) P_0 \eta_0 T. \quad (5)$$

In this approximation, the specific heat is essentially linear in T since $\eta_0 = \eta(E = 2.4 kT)$ is only slightly temperature dependent. The magnitude of C_{ex} may depend on the time scale of the heat-capacity measurement through η_0 .

The phonon thermal conductivity κ may be obtained from

$$\kappa = \frac{1}{3} \sum_i \int_0^{\omega_{i, \max}} d\omega C_i(\omega) v_i l_i(\omega), \quad (6)$$

where $C(\omega)$ is the contribution to the phonon specific heat of phonons having angular frequency ω and mean free path l . If phonons are indeed scattered by tunneling states, the model provides two contributions to $l(\omega)$: a resonant scattering pro-

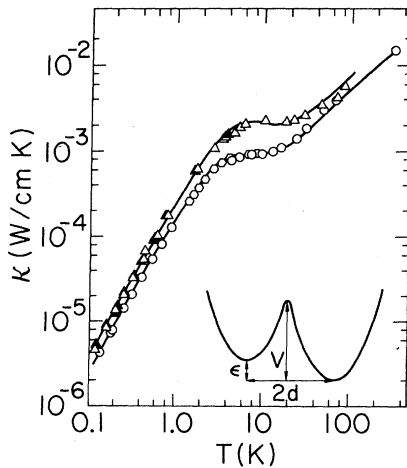


FIG. 1. Thermal conductivity of vitreous silica. Δ —neutron irradiated, 10 day; \blacktriangle —neutron irradiated, 30 day; \circ —unirradiated; hexagon, —unirradiated, Ref. 48. The solid lines are calculated from the tunneling-states model. The inset shows the form of the potential well used in this model.

cess and a relaxation process. The resonant process occurs when a phonon of frequency ω is absorbed by a state of energy $E = \hbar\omega$ and later reradiated in a different direction,^{11,12,21,28}

$$l_{i,\text{res}}^{-1} = \left(\frac{2\gamma^2}{\rho v^2} \right)_i \frac{\pi}{2\hbar v_i} E \tanh \left(\frac{E}{2kT} \right) \times \int_{\tau_{\min}}^{\tau_{\max}} d\tau \left(\frac{\Delta}{E} \right)^2 P(E, \tau) \quad (7)$$

$$= (2\gamma^2/\rho v^2)_i (\pi/2\hbar v_i) E \tanh(E/2kT) P(E). \quad (8)$$

Note that $\eta(E)$ is missing from this expression. The integral over τ has selected the fraction of states with short relaxation times as the most important scatterers. The relaxation process involves all energies E ,^{21,28}

$$l_{i,\text{rel}}^{-1} = \left(\frac{2\gamma^2}{\rho v^2} \right)_i (4kT v_i)^{-1} \int_0^{E_{\max}} dE P(E) \text{sech}^2 \left(\frac{E}{2kT} \right) \times \int_{\tau_{\min}}^{\tau_{\max}} d\tau \frac{(1 - \tau_{\min}/\tau)^{1/2} \omega^2}{(1 + \omega^2 \tau^2)} \quad (9)$$

With $P(E) = P_0$ and in the high-frequency limit ($\omega \tau_{\min} \gg 1$), Eq. (9) may be integrated,

$$l_{i,\text{rel}}^{-1} = \left(\frac{2\gamma^2}{\rho v^2} \right)_i (\hbar^4 \pi v_i)^{-1} \sum_j \left(\frac{2\gamma^2}{\rho v^2} \right)_j \left(\frac{kT}{v_j} \right)^3 P_0. \quad (10)$$

The mean free path to be substituted into the thermal conductivity integral, Eq. (6), is then $l_i = (l_{i,\text{res}}^{-1} + l_{i,\text{rel}}^{-1})^{-1}$. For temperatures $T \lesssim 1$ K, the resonant term tends to dominate. If $P(E) = P_0$, the resulting temperature dependence at low temperatures is simply $\kappa \propto T^2$.

Ultrasonic attenuation is given by $l_i^{-1} = l_{i,\text{res}}^{-1} + l_{i,\text{rel}}^{-1}$ provided the acoustical intensity is sufficiently small. Otherwise, states resonant with the applied frequency ω_0 become equally populated and the term $l_{i,\text{res}}^{-1}$ goes to zero.^{12,28,30,31} The variation Δv_i of ultrasonic phonon velocity with changes in temperature can be obtained³² from the attenuation using the Kramers-Kronig relation,

$$(\Delta v/v)_i = [v_i(T) - v_i(T_0)]/v_i(T_0) \quad (11)$$

$$= \left(\frac{v_i}{\pi} \right) \int_0^{\omega_i, \max} d\omega (\omega_0^2 - \omega^2)^{-1} \times [l_i^{-1}(T, \omega) - l_i^{-1}(T_0, \omega)], \quad (12)$$

where T_0 is a fiducial temperature. This result applies to large acoustical intensities²¹ and is therefore readily measured.

For a density of states independent of E , we have noted that, essentially, $C \propto T$ and $\kappa \propto T^2$. These are nearly, but not exactly, the temperature dependences observed experimentally, and an en-

ergy-dependent $P(E)$ was suggested³³ to account for the differences. The same situation exists for acoustical and Brillouin scattering measurements.^{34,35} Therefore, anticipating the discussion presented in Sec. IV, we assume a form of $P(E, \tau)$ such that

$$\eta(E)P(E) = \begin{cases} P_m(E/kT_N)^m + P_n(E/kT_N)^n & \text{for } E < E_{\max} \\ 0 & \text{for } E > E_{\max} \end{cases} \quad (13)$$

$$\quad (14)$$

The energy E has been normalized by dividing by kT_N where $T_N = 1$ K. The coefficients P_m and P_n are constants, and m and n are roughly 0.3 and 3, respectively, for fused silica. This certainly is not a unique representation of $P(E)$, but it does provide reasonable agreement with the experimental measurements while still being mathematically convenient. The specific heat, for example, takes on the form

$$C_{\text{ex}} = k^2 P_m \Gamma(3+m) Z(2+m) T^{1+m} + k^2 P_n \Gamma(3+n) Z(2+n) T^{1+n}, \quad (15)$$

where $Z(x) = 1 - 2^{-x} + 3^{-x} - 4^{-x} \dots$

It has been suggested³⁶ that some tunneling states may be associated with impurities since the presence of OH^- in vitreous silica apparently alters C_{ex} and κ . A factor of 200 increase in OH^- content is accompanied by an increase³⁷ in C_{ex} by a factor of 1.5. It has not been established whether the changes arise through the introduction of new localized states by the OH^- , through the influence of OH^- on preexisting states, or through different thermal histories of the glasses having different OH^- levels. Whatever the cause, the densities of states of all glasses, pure and impure, show both a broad distribution in E and an apparent distribution³⁷ in τ . Since all of our work is on the same vitreous silica, we will represent all the states by a single density of states $P(E, \tau)$:

$$P(E, \tau) = P(E, \tau)_{\text{pure}} + P(E, \tau)_{\text{impurities}}. \quad (16)$$

Obviously, other samples may possess entirely different $P(E, \tau)$ depending on their composition and history.

Recently, it has also been suggested³⁸ that there are "anomalous" tunneling states in vitreous silica which contribute only to C_{ex} . Analysis of our data does not require this assumption (see Appendix). Occasional reference is made³⁹ to the fraction of states which strongly scatter phonons. This has already been included here as the factor η^{-1} [see Eqs. (4) and (8)].

Thus far, the theoretical development has been mostly phenomenological. A complete microscopical theory would provide $P(E, \tau)$ from the de-

tailed atomic configurations intrinsic to amorphous materials. On the other hand, a density of states that can quantitatively account for all experimental data would provide a target for microscopic theories. Hence, it is important to determine if the tunneling model can provide an appropriate $P(E, \tau)$.

III. EXPERIMENTS AND RESULTS

All amorphous systems appear to be similar in their low-temperature properties. However, the exact magnitudes and temperature dependences of these properties differ between different classes of amorphous materials, and even between different samples of the same material such as vitreous silica. Hence, in attempting to compare experimental data with the tunneling-states model or other theory, it is important that all measurements be made on the same specimen.

Our plan was, first, to test the tunneling-states model by asking whether a single density of states $P(E, \tau)$ would be consistent with the data from measurements on several different properties of the same sample. We would then, as a second step, alter the number of localized excitations and see if the tunneling-states model would continue to be consistent with the new sets of experimental data.

Vitreous silica was selected since there was evidence that neutron irradiation would reduce the number of localized excitations (see Sec. I). It should be noted that this reduction is not due to crystallization of the silica within regions of "thermal spikes" caused by the incident neutrons,²³ since mild heat treatment at $\approx 900^\circ\text{C}$ returns the mass density, thermal conductivity,²⁶ and acoustical properties⁴⁰ to those values measured prior to irradiation. In addition, if *only* crystallization

were occurring, the observed changes in mass density and specific heat with irradiation would require that the crystallized material comprise about 30% of the sample. This is not consistent with x-ray studies.²⁴ In fact, the short-range order in vitreous silica is *decreased* on irradiation.^{24,41} Hence, neutron irradiation appears to alter the density of localized excitations through a modification in the amorphous structure.

The samples of vitreous silica, cut from a single piece⁴² of Spectrosil-B, had dimensions of $5 \times 1 \times 0.3$ cm. These samples were divided into three groups. One group was not irradiated, the second was irradiated with an integrated neutron flux of $1.7 \times 10^{19} \text{ cm}^{-2}$ above 0.1 MeV (10-day samples), and the third group was irradiated with an integrated flux of $5 \times 10^{19} \text{ cm}^{-2}$ above 0.1 MeV (30-day samples). During irradiation the samples were wrapped with aluminum foil and placed in air-cooled aluminum canisters as required by the reactor facility. Thus, the samples were not in direct thermal contact with the reactor coolant and certainly were elevated in temperature above their environment. This probably accounts for the fact that both the 10- and 30-day samples had the same mass density (Table I) and thermal properties (reported below). However, it has been suggested that factors in addition to irradiation temperature may be responsible for the observed saturation density.⁴³ Briefly, both groups of irradiated samples attained an equilibrium situation at an elevated temperature in a time interval less than 10 days. It should be noted that the irradiated samples were strained as evidenced by optical birefringence. It is known, however, that strain does not alter the thermal conductivity⁴⁴ or specific heat.⁴⁵ The irradiated samples also

TABLE I. Summary of parameters for vitreous silica either measured directly or deduced from the measurements reported in this paper. All parameters are defined in the text.

Parameter	Units	Unirradiated samples	Irradiated samples
ρ	g/cm^3	2.20	2.24
v_t	cm/sec	5.81×10^5	6.04×10^5
v_t	cm/sec	3.73×10^5	3.73×10^5
t	sec	5	5
$(\hbar\omega_t/k)_{\text{max}}$	K	330	330
$(\hbar\omega_t/k)_{\text{max}}$	K	60	60
l_{max}	cm	3	3
l_{min}	cm	1.5×10^{-7}	1.5×10^{-7}
γ_t	eV	1.17	1.17
P_m	$\text{erg}^{-1} \text{cm}^{-3}$	1.04×10^{33}	6.9×10^{32}
m	...	0.35	0.33
P_n	$\text{erg}^{-1} \text{cm}^{-3}$	9.8×10^{29}	2.6×10^{29}
n	...	3.3	3.3
E_{max}/k	K	38	53

exhibited a faint bluish coloration.

Following irradiation, the samples were etched to remove radioactive contamination from the surfaces and then allowed to "cool" for one year to further reduce the level of radioactivity present. The self-heating of the 30-day samples after one year was measured to be $\approx 10^{-9}$ W/cm³.

Infrared absorption measurements were made to determine the relative OH⁻ concentration in the three groups of samples, since OH⁻ was the most abundant impurity at ≈ 1000 ppm. We found that neutron irradiation caused no change in the OH⁻ infrared band at 2.73 μ m. This result conflicts with the increase in the 2.73- μ m absorption with irradiation observed in earlier measurements by Primak *et al.*⁴⁶ The conflict might be explained if their samples were immersed in the cooling water of the reactor.

A series of measurements were made on each sample. First, the low-temperature ($T \lesssim 2$ K) thermal conductivity was measured using the entire sample. Then a section $1 \times 1 \times 0.3$ cm was cutoff for use in high-temperature ($T \gtrsim 2$ K) thermal conductivity measurements. This kept the thermal time constant of the sample at a reasonable value. Finally, a section $0.3 \times 0.5 \times 1.5$ cm was removed for use in specific heat and velocity of sound measurements.

The low-temperature thermal conductivity was measured using a two-thermometer technique wherein one end of the sample is heated, the other end is heat sunk, and the resulting temperature gradient is measured by two precalibrated Ge resistance thermometers. Thermometers could not be calibrated *in situ* because of the "background" temperature gradient created by residual heating from radioactive decay. In the high-temperature measurements, one square face of the sample was bonded to a copper plate maintained at a constant temperature, while a second copper plate containing an electrical heater and Ge thermometer was bonded to the opposite face. One measurement was made at 300 K on the unirradiated glass sample using a commercial thermal comparator.⁴⁷

The thermal-conductivity data are presented in Fig. 1. The uncertainty in the κ measurements is $\lesssim 3\%$. For the unirradiated samples, both the low- and high-temperature data are in good agreement with previous measurements.^{1,33,48} Data for similar (synthetic) silica glasses measured by Damon⁴⁸ are included in Fig. 1 for comparison. Below $T \approx 1$ K the data are well represented by the empirical relations (in units of W/cm K)

$$\kappa = (1.61 \pm 0.05) \times 10^{-4} T^{1.81 \pm 0.05}, \quad (17)$$

for the unirradiated samples and

$$\kappa = (2.61 \pm 0.10) \times 10^{-4} T^{1.88 \pm 0.05}, \quad (18)$$

for the 10- and 30-day samples.

The heat-capacity measurements in the region 0.1–1 K were made using a calibrated calorimeter described previously.⁴⁹ The time span of the experiment was ≈ 5 sec. Due to possible drift in the platform calibration, the measurements were repeated in different low-temperature runs and found to be reproducible within the experimental uncertainty. In the region $0.4 < T < 4$ K, the heat capacity was measured by a standard weak-thermal-link technique in which an uncalibrated thermometer and Pt-W alloy heater were glued directly to the sample. The heat capacity was calculated from the magnitude of the temperature pulse produced when a known heat pulse was applied. Also in the region $0.4 < T < 4$ K, the heat capacity was calculated from the measured diffusivity and thermal conductivity. In the regions where all three methods were employed, the data agreed to within the experimental uncertainty. It should be noted that the radioactive self heating of the samples prevented utilization of the weak-thermal-link technique or the diffusivity technique below 0.4 K.

Some of the specific-heat data are plotted in Fig. 2 as C/T^3 , allowing the high-temperature behavior to be studied more easily. The uncertainty in the specific-heat data is estimated to be $\lesssim 10\%$. Data for the unirradiated samples are in good agreement with earlier measurements.^{33,45} Below ≈ 0.6 K the data are well represented by the empir-

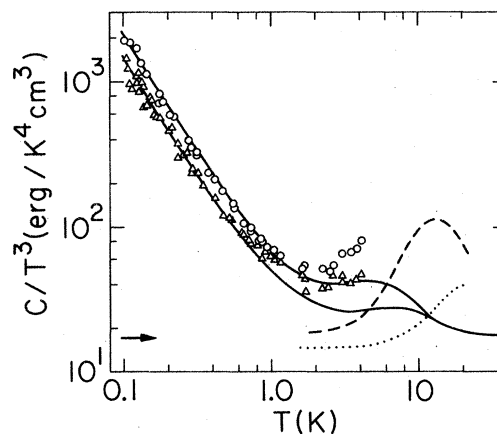


FIG. 2. Specific heat of vitreous silica divided by the cube of the temperature. Δ —neutron irradiated, 10-day; \circ —unirradiated. The 30-day data have been omitted for clarity. The solid lines are calculated from the tunneling-states model. Also shown are the specific heat of crystalline quartz (dotted line) and cristobalite (dashed line) from Ref. 52. The arrow indicates the calculated phonon contribution to the specific heat of vitreous silica [Eq. (21)].

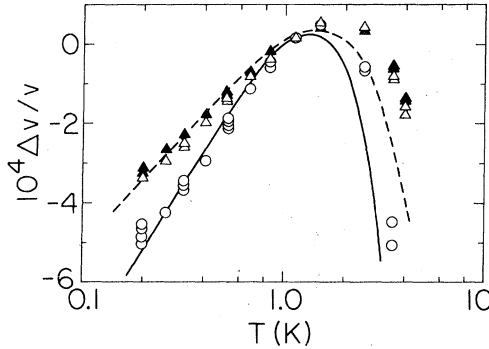


FIG. 3. Variation of the transverse acoustic velocity with temperature in vitreous silica at 5×10^7 Hz. Δ —neutron irradiated, 10-day; \blacktriangle —neutron irradiated, 30-day; \circ —unirradiated. The lines were calculated from the tunneling-states model: solid for unirradiated and broken for irradiated. The calculated velocity variations have been normalized to 0 and 10^{-5} at 1 K for the unirradiated and irradiated samples, respectively.

ical relations (in units of $\text{erg}/\text{cm}^3\text{K}$)⁵⁰

$$C = (46.0 \pm 2.3) T^{1.35 \pm 0.05}, \quad (19)$$

for the unirradiated samples and

$$C = (39.5 \pm 3.8) T^{1.49 \pm 0.12}, \quad (20)$$

for 10- and 30-day samples.

Measurements of the variation of acoustical velocity with changes in temperature were measured using a pulse-echo overlap technique.⁵¹ The measuring frequency was 5×10^7 Hz for both the transverse and longitudinal modes of propagation. The results are presented in Figs. 3 and 4. Data from the unirradiated samples agree with earlier measurements^{32,34} to an experimental uncertainty of 5%.

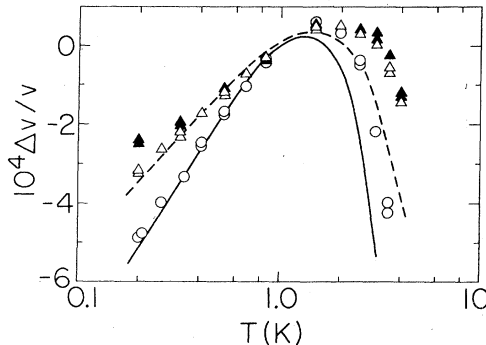


FIG. 4. Variation of the longitudinal acoustical velocity with temperature in vitreous silica at 5×10^7 Hz. Notation is the same as Fig. 3. The lowest temperature data for the 30-day sample (\blacktriangle) are in error due to heating of the sample by radioactive decay. This was avoided in later runs by improved thermal contact to the sample.

IV. DISCUSSION

First, we look at the data in a qualitative manner without recourse to theory. We do assume, based on experimental evidence,² that heat is transported primarily by phonons in the temperature range 0.1–100 K and that the excess specific heat arises from localized excitations.

The excess specific heat C_{ex} is obtained from the measured specific heat by subtracting the Debye phonon contribution C_{ph} ,

$$C_{\text{ph}} = 4.1 \times 10^{17} T^3 \sum_i v_i^{-3}, \quad (21)$$

in units of $\text{erg cm}^{-3} \text{K}^{-1}$. In the temperature range 0.1–1 K, the decrease in C_{ex} between neutron-irradiated (I) and unirradiated (U) samples is given by the ratio

$$C_{\text{ex}}(I)/C_{\text{ex}}(U) = 0.73 \pm 0.11, \quad (22)$$

which would indicate roughly a 30% reduction in the number of localized excitations. This may be compared with the corresponding increase upon irradiation in the thermal conductivity below 1 K,

$$\kappa(U)/\kappa(I) = 0.62 \pm 0.06, \quad (23)$$

and a reduction, below 1 K, in the temperature dependences of the transverse ultrasonic velocity,

$$[\Delta v(I)/v]/[\Delta v(U)/v] = 0.61 \pm 0.06, \quad (24)$$

and the longitudinal ultrasonic velocity,

$$[\Delta v(I)/v]/[\Delta v(U)/v] = 0.68 \pm 0.07. \quad (25)$$

The most simple interpretation of the results presented in Eqs. (22)–(25) is that each change below 1 K has been caused by the same $\approx 35\%$ reduction in the density of localized excitations. This strongly suggests that no mechanism^{3,13,17–20} is required to explain the T^2 dependence of the phonon thermal conductivity other than scattering from the localized excitations responsible for C_{ex} .

Above 1 K, the specific heat also decreases with neutron irradiation (Fig. 2 and Ref. 27). Discussion of this effect, however, is complicated by an uncertainty in the phonon contribution. Crystalline materials show strong deviations from T^3 Debye behavior above 1 K. The specific heats of quartz and cristobalite⁵² are shown in Fig. 2 as examples. If a similar dispersion-enhanced specific heat is present in glasses, as is possibly the case,⁵² the phonon contribution to the measured specific heat would be unknown and C_{ex} could not be extracted.

The plateau in the thermal conductivity above 1 K (Fig. 1) is caused^{1,2} by a highly frequency-dependent mean free path $l(\omega)$ for $\omega \gtrsim 10^{12} \text{ sec}^{-1}$. The phonon scattering causing this plateau is often as-

cribed^{11, 17, 18, 20} to a Rayleigh process

$$l(\omega) = A^{-1} \omega^{-4}, \quad (26)$$

arising from fluctuations in mass density and elastic constants. As a result of this highly frequency-dependent scattering, an inordinately large proportion of the thermal transport at 10 K is provided by phonons having wavelengths long² compared to those characteristic of a temperature of 10 K. If neutron irradiation left A in Eq. (26) unchanged, the increased mean free path of the long-wavelength phonons alone would only provide an increase of a factor of ≈ 1.6 in κ in the plateau region, just as for $T < 1$ K [Eq. (23)]. The observed increase is a factor of 2.5, however, implying that A and hence the related phonon scattering must decrease by a factor of ≈ 1.6 upon irradiation. The decrease in A does not appear to be consistent with experimental data, since atomic disorder^{24, 41} and density fluctuations⁵³ are reported to increase with irradiation. We will thus assume in later calculations that the highly frequency-dependent mean free path causing the plateau is related to the localized excitations⁵⁴ rather than a Rayleigh process.

Neutron irradiation reduces the temperature dependences of the ultrasonic velocities above 1 K (Figs. 3 and 4). However, the narrow experimental temperature range precludes a more definitive discussion.

Our qualitative analysis of the data has indicated that the localized excitations observed in the specific heat are also responsible for the anomalous thermal conductivity of vitreous silica at temperatures up to ≈ 10 K and the temperature dependence of the ultrasonic velocities at least for temperatures below ≈ 1 K.

We next compare the experimental data quantitatively with the equations derived from the tunneling-states model in Sec. II. This involves obtaining a density of states $P(E)$ and other parameters consistent with all of our measurements on the unirradiated glass. We then change only $P(E)$ in the model to account for data from the neutron-irradiated samples.

There are first a number of parameters to be discussed that are either well determined experimentally or are not used as adjustable fitting parameters. The mass density ρ and the transverse and longitudinal phonon velocities, v_t and v_l , were measured on our samples to 2%. The quantity $\eta(E)$ is not a separate parameter but is uniquely determined by other parameters [Eq. (4)]. The time scale t of the specific-heat experiment enters the quantity $\eta(E)$ only logarithmically and thus is adequately determined. (See the Appendix for a detailed discussion of time scales, τ_{\max} ,

and C_{ex} .)

The upper limits $\omega_{i, \max}$ (Eq. 6) on the three-phonon spectra are taken to be those of crystalite, since this appears to be the best approximation presently available.⁵³ The total mean free path l_i for the thermal conductivity integral [Eq. (6)] has the form

$$l_i = l_{\min} + (l_{\max}^{-1} + l_{i, \text{res}}^{-1} + l_{i, \text{rel}}^{-1})^{-1}, \quad (27)$$

where $l_{i, \text{res}}$ and $l_{i, \text{rel}}$ are from Eqs. (8) and (9). The term l_{\max} is taken to be roughly the length of the sample and serves only to permit integration from $\omega = 0$. It effects κ most strongly at low temperatures, but then only by $\approx 1\%$ at 0.1 K.

Finally, the normalized phonon-coupling parameters $(2\gamma^2/\rho v^2)_i$ in Eqs. (1), (8), and (9) are assumed to have the same value²¹ for both longitudinal and transverse waves. This assumption is justified because the measured $(\Delta v/v)_i$ are the same for the two modes and, as can be seen from Eqs. (8) and (12), any difference between the $(\Delta v/v)_i$ curves for the two modes at low temperatures should arise from the normalized coupling parameters $(2\gamma^2/\rho v^2)_i$. The values of the fixed parameters ρ , v_t , t , $\omega_{i, \max}$, and l_{\max} are given in Table I.

Seven parameters (P_m , m , P_n , n , E_{\max} , γ_l , and l_{\min}) are considered to be variable in the fitting procedure. The term l_{\min} in Eq. (27) is the shortest conceivable mean free path for phonons, of the order of a few angstroms, as discussed by Kittel.⁵⁵ It effects only κ and only above 10 K. (Changing the estimates for $\omega_{i, \max}$ would merely require a corresponding change in l_{\min} to keep the same κ between 10 and 100 K.)

Ideally, the five parameters involved in the density of states [Eq. (13)] would be determined by the specific heat only. Then γ_l and l_{\min} would be determined by the low- and high-temperature thermal conductivities, respectively. Uncertainties in the magnitude of C_{ex} at high temperatures, however, make necessary a different fitting procedure. Two parameters, P_m and m , and the value of the normalized coupling constant $(2\gamma^2/\rho v^2)$ are adjusted to give the magnitudes and temperature dependences of both the specific heat and thermal conductivity below ≈ 1 K. (Note that the three adjustable parameters are overdetermined by the four measured parameters.) Then P_n , n , E_{\max} , and l_{\min} are adjusted to give agreement with the thermal conductivity at higher temperatures. The values of the adjusted parameters are listed for the unirradiated glass in the lower half of Table I.

The results of the fitting to the thermal-conductivity data for the unirradiated samples is shown as the solid line in Fig. 1. The calculated

phonon contribution to the specific heat [Eq. (21)] plus that calculated for the tunneling states [Eq. (15)] is shown in Fig. 2 for the unirradiated glass. The only major discrepancy between the calculations and the data occurs in the specific heat above 1 K. However, this may be due to phonons of high dispersion, as in cristobalite, as discussed above. Since the size of this effect is undetermined, the density of states at large energies cannot be deduced from the specific heat.

The tunneling-states model thus can provide good agreement with the measured specific heat from 0.1 to 1–2 K, and with the measured thermal conductivity from 0.1 to 300 K. Note again that only those states appearing explicitly in Eq. (13) are required to explain the data—no additional or special excitations need to be introduced. As a test of the model, the adjusted parameters are left fixed in the calculation of the temperature dependences of the transverse and longitudinal ultrasonic velocities. The results are shown in Figs. 3 and 4 as the solid curves. The agreement with data is excellent below 1 K. Above 1 K, the calculation provides an especially sensitive test of the fitting parameters, since the resonant and relaxation contributions to $\Delta v/v$ have opposite sign and are in strong competition. The discrepancy between calculation and data above 1 K would be removed by a 15% decrease in the relaxation contribution. There is no parameter available, however, to adjust the relative magnitudes of the relaxation and resonant contributions under our assumptions for the tunneling-states model.⁵⁶

As a further test, the data for the neutron-irradiated glass are fitted by changing only the parameters found in the density of states $P(E)$. The results, shown in Figs. 1–4, have the same quality of agreement to the data as for the unirradiated glass. The required values of the changed parameters are listed near the bottom of Table I. Note that, effectively, only three parameters, E_{\max} , P_m , P_n , are changed to produce the measured difference between the irradiated and unirradiated samples.

In order to facilitate comparison between our fit and the experimental data, the decrease ΔW in the thermal resistivity $W = \kappa^{-1}$ caused by neutron irradiation is shown in Fig. 5, normalized to the value of W for the unirradiated sample. The solid line is calculated using the difference between $P(E)$ for the irradiated and for the unirradiated glass (Table I).

One final test of the model can be made by comparing our deduced values for phonon mean free paths with measurements reported in the literature for similar glasses. Figure 6 shows, at five temperatures, the longitudinal phonon mean free

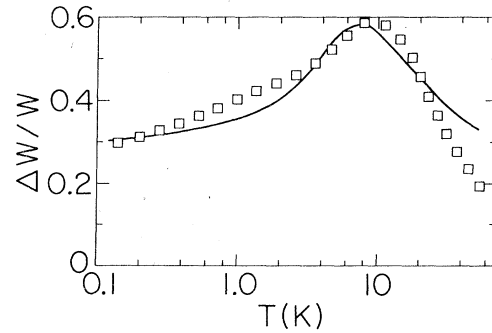


FIG. 5. Reduction ΔW in thermal resistivity W of vitreous silica caused by neutron irradiation. The squares represent the experimental results obtained from smooth curves drawn through the thermal conductivity data. The solid line is the calculated reduction in thermal resistivity based on the two densities of states discussed in the text.

paths calculated using Eqs. (8), (9), and (27), and parameters for unirradiated glass as given in Table I. Also shown at low frequencies are direct ultrasonic determinations^{39,57-59} of l and, at $\hbar\omega/k > 1$, data derived from Brillouin scattering experiments.^{35,60,61} Agreement with the calculated values is good in light of the strong dependence on both frequency and temperature. However, at 10 K and above, the calculated mean free paths are probably only approximations to the actual mean free paths which, when averaged over ω , produce the correct thermal conductivity. Phonon scattering processes other than l_{res} and l_{rel} need to be considered,⁵⁷ and the abrupt cutoff in $P(E)$ assumed to occur at E_{\max} is unphysical.

The values of the parameters used in the density of states are reasonable. For example, if the tunneling entity were an oxygen atom tunneling through distances of $2d \approx 0.1$ – 1.0 Å and barriers of height $V \approx 0.1$ – 0.6 eV (Fig. 1), there would be states with energies as large as $E_{\max} \approx 50$ K. Also, the total number of states N with relaxation times less than 5 sec,

$$N = \int_0^{E_{\max}} \eta(E) P(E) dE, \quad (28)$$

is $\approx 2 \times 10^{20}/\text{cm}^3$, or 0.1% of the oxygen atoms, for both the irradiated and unirradiated samples.

Finally, the phonon coupling parameter γ_i has been measured independently of other parameters in a phonon echo experiment,²² but for a different glass and with a large uncertainty. The phonon echo experiment gave $\gamma_i = 1.6$ eV as compared to our fitted value of 1.17 eV.⁶² Additional discussion on limiting values for γ may be found in the Appendix.

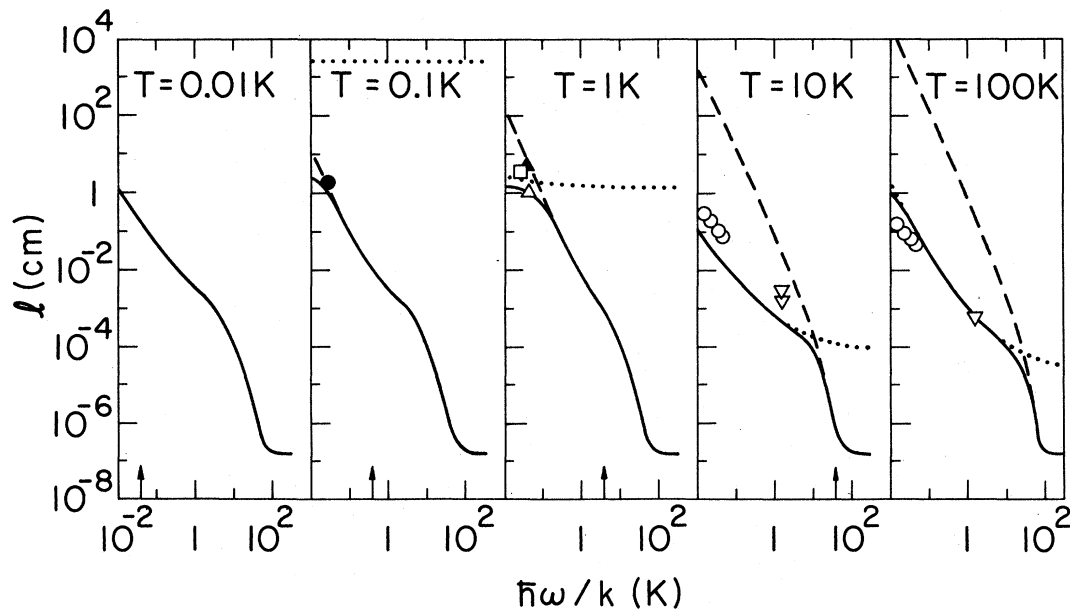


FIG. 6. Longitudinal phonon mean free paths used in fitting the thermal conductivity and ultrasonic velocity data for unirradiated vitreous silica vs phonon frequency at several temperatures. Dashed line, l_{res} [Eq. (8)]; dotted line, l_{rel} [Eq. (9)]; solid line, total l [Eq. (27)]. The data points are measured l values as described in the text: \bullet , l_{res} (Ref. 39); \blacktriangle , l_{res} (Ref. 58); Δ , $(l_{\text{res}}^{-1} + l_{\text{rel}}^{-1})^{-1}$ (Ref. 58); \square , l_{rel} (Ref. 57); \circ , l_{rel} (Ref. 59); ∇ , l_{rel} (Refs. 35, 60, and 61). The arrows indicate the frequencies of maximum phonon contribution to the specific heat at each temperature (i.e., the "dominant" phonons).

V. SUMMARY

Neutron irradiation of vitreous silica produces changes of the same relative magnitude in the low-temperature excess specific heat C_{ex} , the anomalous thermal conductivity κ , and the anomalous temperature dependence of ultrasonic velocity $\Delta v/v$. It is therefore likely that κ and $\Delta v/v$ are dominated by the localized excitations responsible for the excess specific heat of amorphous materials.

The tunneling-states model can quantitatively account for the measured C_{ex} , κ , and $\Delta v/v$ of unirradiated vitreous silica using an energy-dependent density of states. No additional "impurity" or "anomalous" states are required nor are other phonon-scattering mechanisms needed. This is true for κ even above the temperatures for which the model was designed. In addition, the changes in C_{ex} , κ , and $\Delta v/v$ upon neutron irradiation are explained by altering only the density of tunneling states. The simplifying assumptions used in the density of states and in the model need to be investigated further. Also, these results may not extrapolate to other types of amorphous materials or, perhaps, even to other types of vitreous silica.

In conclusion, it should be noted that this experiment was not undertaken with the defense of the tunneling-states model in mind. Rather,

it was meant as a further test of the model, i.e., as another set of experimental measurements which must be accounted for by any model designed to explain the properties of amorphous materials.

VI. ACKNOWLEDGMENTS

This work was supported in part by the NSF under Grant No. DMR 77-08599, and by the U.S. ERDA under contract No. EY-76-C-02-1198. We are indebted to J. R. Matey for arranging the neutron irradiation at the CP-5 reactor, Argonne National Laboratories, and to R. E. Taylor and H. Groot for the use of a thermal comparator.

APPENDIX

One of the early predictions of the tunneling-states model was that the measured specific heat should vary logarithmically with the time scale of the experiment¹⁰ [Eq. (4)]. However, this depends on the implicit assumption that there are double-well potentials for which the relaxation time τ is longer than the experimental time scale. It is conceivable that there are glasses with constraints on the parameter λ (and thus on Δ and τ_{max}) such that the distribution in τ is not tens of orders of magnitude broad. Yet even a restricted distribution in τ should show a measurable time-

TABLE II. Decrease ΔC in specific heat measured on a time scale of 5×10^{-5} sec relative to a specific heat C measured on a 5-sec time scale, divided by C , at low temperatures for several values of τ_{\max} . Parameter $\gamma_i = 1.17$ eV.

τ_{\max} (sec)	$\Delta C/C$ (1 K) (%)	$\Delta C/C$ (0.1 K) (%)
≥ 5	35	65
5×10^{-1}	31	60
5×10^{-2}	26	53
5×10^{-3}	19	43
5×10^{-4}	11	28
5×10^{-5}	0	0

dependent specific heat if the shortest time-scale experiment is faster than τ_{\max} .

For example, Table II shows, for several values of τ_{\max} , the percentage decrease $\Delta C/C$ expected for an experiment having a time scale of 5×10^{-5} sec, compared to the 5-sec time scale experiments on our glass. For temperatures ≥ 1 K, the increasing importance of the thermal phonon contribution to the specific heat masks the time-dependent change in the excess specific heat, especially if there is an excess phonon specific heat as discussed in Sec. IV.

An experiment to measure heat capacity on a $\approx 10^{-4}$ sec time scale was attempted by Goubau and Tait.⁶³ At 0.1 K they observed no time-dependent specific heat. At about 1 K they found a change, though smaller than they expected. [However, this result at 1 K is in rough agreement with the change we would expect using our glass parameters and a $\tau_{\max} \geq 5$ sec (see Table II)]. At temperatures above 2 K, no conclusions can be drawn from their measurements since no long-time specific-heat experiments were done on the same glass at those temperatures for comparison.

The apparent problem in explaining these data using the tunneling-states model provoked alternate analyses of the raw data. The most appropriate solution has been given by Black,³⁸ who finds it necessary to introduce "anomalous" excess excitations. This analysis makes use of a local-temperature approximation which may be invalid because of the strong frequency dependence of the phonon mean free path. Thus, the initial phonon-frequency spectrum and the resulting thermal history of the sample will depend on how a heat pulse is applied⁶⁴ (i.e., if by an electrical heater or other means), and on the magnitude and duration of the heating pulse.

We feel, however, that the Goubau and Tait experiment has not shown any discrepancy with the tunneling-states model and no revisions are needed

TABLE III. Values of the coupling parameter γ_i required by the experimental data below 1 K in this paper if the maximum relaxation time of the localized excitations is τ_{\max} .

τ_{\max} (sec)	γ_i (eV)
≥ 5	1.17
5×10^{-1}	1.10
5×10^{-2}	1.02
5×10^{-3}	0.94
5×10^{-4}	0.85
5×10^{-5}	0.75

as yet. First, at the lowest temperatures (0.1 K) the data were not corrected⁶⁵ for the heat capacity⁶⁶ of the manganin heater which, if 100 Å thick, would itself have as much heat capacity as that expected for the glass on a time scale of 5×10^{-5} sec. Second, the data obtained from the experiment should be plotted⁶⁷ near $T + 1.6T_m$, rather than⁶⁵ at $T + 0.5\Delta T_m$, because of the higher-temperature history of the bulk of the sample. For $\Delta T_m/T = 10\%$ this introduces an 11% error in C at temperatures where C is nearly linear in T and a 37% error in C where C is proportional to T^3 . Finally, the values of C obtained from the experimental procedure used in Ref. 63 are very dependent⁶⁸ on heating methods and heat losses. Based on the geometry⁶⁵ of the experiment, we expect errors on the order of 5%. All the above problems apply independently of the method used to calculate C from the raw data and, if corrected for, tend to provide a greater disparity between long-time scale and short-time scale values.

Thus, at present, there appears to be no discrepancy between experiment and theory for vitreous silica. Should some future specific-heat experiment done on a fast time scale precisely show only a fraction of the change expected, this still may not drastically effect the fit and conclusions of Sec. IV. For instance, a change of $\approx 50\%$ observed at 0.1 K for our glass in a 5-sec vs 5×10^{-5} -sec experiment might be due to a τ_{\max} of only 5×10^{-2} sec as indicated in Table II. In this case, because of the logarithmic dependence on τ_{\max} , the value of γ_i need change⁶⁹ only from 1.17 to 1.02 eV to retain the same fits at low temperatures for C , κ , and $\Delta v/v$. Other values of γ_i required to compensate for given values of τ_{\max} are listed in Table III. Finally, as Black's calculation indicates,³⁸ it does appear possible to account for any future experimental discrepancy by manufacturing a more complicated density of states $P(E, \tau)$ than used in the present paper.

- ¹R. C. Zeller and R. O. Pohl, Phys. Rev. B 4, 2029 (1971).
- ²M. P. Zaitlin and A. C. Anderson, Phys. Rev. B 12, 4475 (1975).
- ³P. Fulde and H. Wagner, Phys. Rev. Lett. 27, 1280 (1971).
- ⁴H. B. Rosenstock, J. Non-Cryst. Solids 7, 123 (1972).
- ⁵S. Takeno and M. Goda, Prog. Theor. Phys. 48, 1468 (1972).
- ⁶H. P. Baltes, Solid State Commun. 13, 225 (1973).
- ⁷L. S. Kothari and Usha, J. Non-Cryst. Solids 15, 347 (1974); Solid State Commun. 15, 579 (1974).
- ⁸P. R. Couchman, C. L. Reynolds, and R. M. J. Cotterill, Nature 264, 534 (1976).
- ⁹W. H. Tanttilla, Phys. Rev. Lett. 39, 554 (1977).
- ¹⁰M. von Schickfus and S. Hunklinger, J. Phys. C 9, L439 (1976).
- ¹¹P. W. Anderson, B. I. Halperin, and C. M. Varma, Philos. Mag. 25, 1 (1972).
- ¹²W. A. Phillips, J. Low Temp. Phys. 7, 351 (1972).
- ¹³G. K. Chang and R. E. Jones, Phys. Rev. 126, 2055 (1962).
- ¹⁴P. G. Klemens, in *Physics of Non-Crystalline Solids*, edited by J. A. Prins (North-Holland, Amsterdam, 1965), p. 162.
- ¹⁵B. Dreyfus, N. C. Fernandes, and R. Maynard, Phys. Lett. A 26, 647 (1968).
- ¹⁶T. Scott and M. Giles, Phys. Rev. Lett. 29, 642 (1972).
- ¹⁷G. J. Morgan and D. Smith, J. Phys. C 7, 649 (1974).
- ¹⁸D. Walton, Solid State Commun. 14, 335 (1974).
- ¹⁹M.-S. Lu and M. Nelkin, Report No. 2415 of the Materials Science Center, Cornell University, 1975 (unpublished); M.-S. Lu, Ph.D. thesis (Cornell University, 1975) (unpublished).
- ²⁰D. Walton, Phys. Rev. B 16, 3723 (1977).
- ²¹S. Hunklinger and W. Arnold, in *Physical Acoustics*, edited by W. P. Mason and R. N. Thurston (Academic, New York, 1976), Vol. 12, p. 155, and papers cited therein.
- ²²B. Golding and J. E. Graebner, Phys. Rev. Lett. 37, 852 (1976).
- ²³W. Primak, *The Compacted States of Vitreous Silica* (Gordon and Breach, New York, 1975), and work cited therein. A brief review of the low-temperature properties of vitreous silica is given by S. Brawer, Phys. Chem. Glasses 16, 2 (1975).
- ²⁴A. J. Leadbetter and A. C. Wright, Phys. Chem. Glasses 18, 79 (1977), and papers cited therein.
- ²⁵After the present paper was submitted, we learned that the same conclusion had been reached on the basis of ultrasonics measurements by C. Laermans, L. Piché, W. Arnold, and S. Hunklinger, in *Physics of Non-Crystalline Solids*, edited by G. H. Frischat (Trans Tech, Aedermannsdorf, Switzerland, 1977), p. 562.
- ²⁶A. F. Cohen, J. Appl. Phys. 29, 591 (1958); J. H. Crawford and A. F. Cohen, Bull. Int. Instrum. Ref. 1, 165 (1958). (These thermal-conductivity data appear to be in error by a factor of ≈ 4 .)
- ²⁷G. K. White and J. A. Birch, Phys. Chem. Glasses 6, 85 (1965), and papers cited therein.
- ²⁸J. Jäckle, Z. Phys. 257, 212 (1972).
- ²⁹J. L. Black and B. I. Halperin, Phys. Rev. B 16, 2879 (1977).
- ³⁰S. Hunklinger, W. Arnold, S. Stein, R. Nava, and K. Dransfeld, Phys. Lett. A 42, 253 (1972).
- ³¹B. Golding, J. E. Graebner, B. I. Halperin, and R. J. Schutz, Phys. Rev. Lett. 30, 223 (1973).
- ³²L. Piché, R. Maynard, S. Hunklinger, and J. Jäckle, Phys. Rev. Lett. 32, 1426 (1974).
- ³³J. C. Lasjaunias, A. Ravex, M. Vandorpe, and S. Hunklinger, Solid State Commun. 17, 1045 (1975), and papers cited therein.
- ³⁴B. Golding, J. E. Graebner, and A. B. Kane, Phys. Rev. Lett. 37, 1248 (1976).
- ³⁵J. Pelous and R. Vacher, J. Phys. (Paris) 38, 1153 (1977).
- ³⁶R. B. Stephens, Phys. Rev. B 8, 2896 (1973); 13, 852 (1976).
- ³⁷S. Hunklinger, L. Piché, J. C. Lasjaunias, and K. Dransfeld, J. Phys. C 8, L423 (1975).
- ³⁸J. L. Black (unpublished).
- ³⁹B. Golding, J. E. Graebner, and R. J. Schutz, Phys. Rev. B 14, 1660 (1976).
- ⁴⁰R. E. Strakna, Phys. Rev. 123, 2020 (1961).
- ⁴¹V. W. Sigaev, A. A. Lashmanov, I. I. Yamzin, L. M. Lenda, and I. N. Kikolaev, Sov. Phys.-Crystallogr. 22, 231 (1977).
- ⁴²Thermal American Fused Quartz Company, Change Bridge Road, Montville, N. J.
- ⁴³W. Primak, Nucl. Sci. Eng. 65, 141 (1978).
- ⁴⁴T. L. Smith, J. R. Matey, and A. C. Anderson, Phys. Chem. Glasses 17, 214 (1976).
- ⁴⁵L. E. Wenger, K. Amaya, and C. A. Kukkonen, Phys. Rev. B 14, 1327 (1976).
- ⁴⁶W. Primak, L. H. Fuchs, and P. Day, J. Am. Ceram. Soc. 38, 135 (1955).
- ⁴⁷For a discussion of this technique see, for example, R. W. Powell, in *Thermal Conductivity*, edited by R. P. Tye (Academic, New York, 1969), Vol. 2, p. 275.
- ⁴⁸D. H. Damon, Phys. Rev. B 8, 5860 (1973).
- ⁴⁹P. J. Anthony and A. C. Anderson, Phys. Rev. B 16, 3827 (1977).
- ⁵⁰Following recent precedent, we use units of ergs/Kcm³ for specific heat. $1\text{K}=1.38 \times 10^{-16} \text{ erg}=1.38 \times 10^{-23} \text{ J}$
 $=9 \times 10^{-5} \text{ eV}=1.3 \times 10^{11} \text{ rad/sec}$.
- ⁵¹E. P. Papadakis, in *Physical Acoustics*, edited by W. P. Mason and R. N. Thurston (Academic, New York, 1976), Vol. 12, p. 277; Rev. Sci. Instrum. 47, 806 (1976).
- ⁵²N. Billir and W. A. Phillips, Philos. Mag. 32, 113 (1975), and references cited therein.
- ⁵³H. D. Bale, R. F. Shepler, and G. W. Gibbs, J. Appl. Phys. 41, 241 (1970).
- ⁵⁴M. P. Zaitlin and A. C. Anderson, Phys. Status Solidi B 71, 323 (1975).
- ⁵⁵C. Kittel, Phys. Rev. 75, 972 (1949); see, also, G. A. Slack (unpublished).
- ⁵⁶The assumption that the dominant coupling of phonons to the tunneling states is through a modulation of ϵ (Sec. II) reduces the parameters M and D of Ref. 21 to $\gamma \Delta/E$ and $2\gamma \epsilon/E$, respectively.
- ⁵⁷J. Jäckle, L. Piché, W. Arnold, and S. Hunklinger, J. Non-Cryst. Solids 20, 365 (1976).
- ⁵⁸W. Arnold, S. Hunklinger, S. Stein, and K. Dransfeld, J. Non-Cryst. Solids 14, 192 (1974).
- ⁵⁹C. K. Jones, P. G. Klemens, and J. A. Rayne, Phys. Lett. 8, 31 (1964).
- ⁶⁰J. Pelous and R. Vacher, Solid State Commun. 21, 1063 (1976).

- ⁶¹H. E. Jackson, S. Rand, and D. Walton, Solid State Commun. 21, 1063 (1976).
- ⁶²For $\gamma_i = 1.6 \text{ eV} = 1.41\gamma_i$ as in Ref. 22, the calculated value of $\tau_{\min} = 1.2 \times 10^{-4} \text{ sec}$ (not $0.65 \times 10^{-4} \text{ sec}$) at 0.02 K and $6.8 \times 10^8 \text{ Hz}$. For our value of $\gamma_i = 1.17 \text{ eV} = 1.56\gamma_i$, the calculated value of τ_{\min} is $2.8 \times 10^{-4} \text{ sec}$. Measured values of τ_{\min} at 0.02 K and similar frequencies are given in Ref. 22 as $\approx 2.0 \times 10^{-4} \text{ sec}$ and $\approx 2.4 \times 10^{-4} \text{ sec}$.
- ⁶³W. M. Goubau and R. A. Tait, Phys. Rev. Lett. 34, 1220 (1975).
- ⁶⁴See, D. S. Matsumoto, C. L. Reynolds, and A. C. Anderson, Phys. Rev B 16, 3303 (1977).

- ⁶⁵W. M. Goubau (private communication).
- ⁶⁶J. C. Ho, H. R. O'Neal, and N. E. Phillips, Rev. Sci. Instrum. 34, 782 (1963).
- ⁶⁷W. J. Parker, R. J. Jenkins, C. P. Butler, and G. L. Abbot, J. Appl. Phys. 32, 1679 (1961).
- ⁶⁸R. C. Heckman, J. Appl. Phys. 44, 1455 (1973); A. B. Donaldson, *ibid.* 43, 4226 (1972).
- ⁶⁹For C_{ex} to remain unchanged, $P(E, \tau)$ must remain unchanged [Eq. (3)]. For κ and $\Delta v/v$ to remain unchanged at low temperatures, $\sum_i \gamma_i^2 / \ln [4\tau_{\max}/\tau_{\min}(\gamma)]$ must remain constant as γ and τ_{\max} vary [Eqs. (8) and (13)].